Kinetics of Proton-Linked Flavin Conformational Changes in *p*-Hydroxybenzoate Hydroxylase†

Kendra King Frederick‡ and Bruce A. Palfey*

Department of Biological Chemistry, University of Michigan, Ann Arbor, Michigan 48109-0606

Received June 10, 2005; Revised Manuscript Received August 1, 2005

ABSTRACT: *p*-Hydroxybenzoate hydroxylase (PHBH) is an FAD-dependent monooxygenase that catalyzes the hydroxylation of *p*-hydroxybenzoate (pOHB) to 3,4-dihydroxybenzoate in an NADPH-dependent reaction. Two structural features are coupled to control the reactivity of PHBH with NADPH: a proton-transfer network that allows protons to be passed between the sequestered active site and solvent and a flavin that adopts two positions: "in", where the flavin is near pOHB, and "out", where the flavin is near NADPH. PHBH uses the proton-transfer network to test for the presence of a suitable aromatic substrate before allowing the flavin to adopt the NADPH-accessible conformation. In this work, kinetic analysis of the His72Asn mutant, with a disrupted proton-transfer network, showed that flavin movement could occur in the presence or absence of NADPH but that NADPH stimulated movement to the reactive conformation required for hydride transfer. Substrate and solvent isotope effects on the transient kinetics of reduction of the His72Asn mutant showed that proton transfer was linked to flavin movement and that the conformational change occurred in a step separate from that of hydride transfer. Proton transfers during the reductive half-reaction were observed directly in the wild-type enzyme by performing experiments in the presence of a fluorescent pH-indicator dye in unbuffered solutions. NADPH binding caused rapid proton release from the enzyme, followed by proton uptake after flavin reduction. Solvent and substrate kinetic isotope effects showed that proton-coupled flavin movement and reduction also occurred in different steps in wild-type PHBH. These results allow a detailed kinetic scheme to be proposed for the reductive half-reaction of the wild-type enzyme. Three kinetic models considered for substrate-induced isomerization are analyzed in the Appendix.

p-Hydroxybenzoate hydroxylase (PHBH)[1] is an FAD-dependent monooxygenase that catalyzes the oxygenation of *p*-hydroxybenzoate (pOHB) to 3,4-dihydroxybenzoate (*1*). The catalytic cycle is divided into two half-reactions: the reductive half-reaction, during which the flavin prosthetic group is reduced by NADPH, and the oxidative half-reaction, during which the flavin reacts with molecular oxygen to form a flavin C(4a)-hydroperoxide that hydroxylates the bound substrate. In the absence of the substrate, the highly reactive flavin−hydroperoxide intermediate rapidly eliminates toxic hydrogen peroxide. To prevent this, the reductive half-reaction is inhibited by a factor of $\sim 10^5$ in the absence of pOHB (*2*), so that very little flavin hydroperoxide is formed. The enzyme accomplishes this at least in part by testing for the presence of the phenolic oxygen of pOHB before moving the flavin to the pyridine nucleotide for reduction.

An understanding of the intricate mechanism for controlling flavin reduction is beginning to emerge. Two critical dynamic features control reduction: a proton-transfer network involved in recognition of the phenolic oxygen of pOHB and the movement of the isoalloxazine moiety of the flavin from the solvent-sequestered "in" position to the position accessible to the pyridine nucleotide (*3*, *4*, *5*). The active site of PHBH is buried and inaccessible to the solvent when the substrate is bound (*6*). The phenolic oxygen of pOHB makes a hydrogen bond with Tyr201, which in turn makes a hydrogen bond to Tyr385. The network continues through the interior of the protein through two buried water molecules, terminating at the distal His72, effectively connecting the phenolic oxygen of pOHB to the solvent (*7*). In a novel form of substrate recognition, the proton-transfer network facilitates the ionization of the phenolic oxygen of the aromatic ligand (*4*); electrostatic repulsion between the phenolate anion and the carbonyl of Pro293 triggers a movement of the peptide backbone (*8*), allowing the isoalloxazine of the flavin to move from a largely inaccessible position, termed "in", to a solvent-accessible position, termed "out" (Figure 1) (*9*, *10*). If the substrate is not ionizable (e.g., *p*-aminobenzoate), then it remains hydrogen-bonded to the carbonyl of Pro293 and flavin movement does not occur. A pendulum-like movement of the isoalloxazine moiety also occurs in phenol hydroxylase (*11*), suggesting that movement of the flavin to achieve control is a general feature of one-component flavoprotein aromatic hydroxylases. Flavin movement is an elegant solution to satisfy the different require-

† K.K.F. was supported by a University of Michigan UROP fellowship and by NIH Grant GM20877 to David P. Ballou. B.A.P. was supported by NIH Grants GM20877 to David P. Ballou and GM11106 to Vincent Massey.

* To whom correspondence should be addressed. Telephone: (734) 615-2452. Fax: (734) 763-4581. E-mail: brupalf@umich.edu.

‡ Present address: Department of Biochemistry and Molecular Biophysics, University of Pennsylvania, Philadelphia, PA 19104.

[1] Abbreviations: PHBH, *p*-hydroxybenzoate hydroxylase; pOHB, *p*-hydroxybenzoate; NADPD, (4*R*)-[4-^{2}H]NADPH.

10.1021/bi051119t CCC: $30.25
Published on Web 09/14/2005

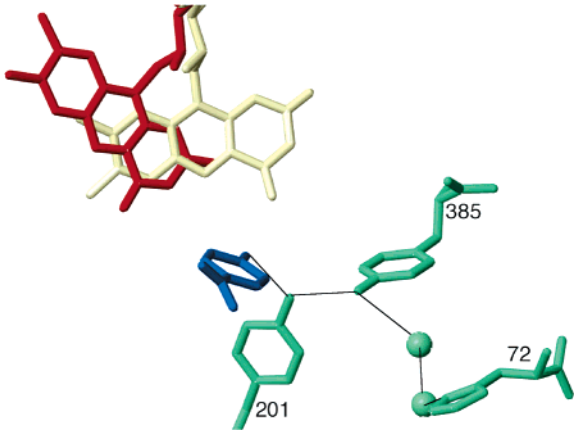

FIGURE 1: Active site of PHBH. The two conformations adopted by the isoalloxazine moiety of the FAD are shown. The "in" form (yellow) is close to the substrate pOHB (blue), seen edge-on in this diagram. The "out" form (red) moves the isoalloxazine toward the exterior of the protein, where it reacts with NAPDH (not shown). Side chains of the proton-transfer network are shown in cyan and connect the phenolic oxygen of the substrate to the exterior of the protein. Coordinates are taken from PDB codes 1IUW ("in") and 1DOE ("out").

ments of the two half-reactions. Reaction with NADPH requires access to the flavin, but once NADP dissociates, it is important to exclude water to prevent side reactions of the unstable intermediates generated in the oxidative half-reaction.

The His72Asn mutant of PHBH has proven invaluable in dissecting the involvement of the proton-transfer network in the control of flavin reduction (*4*, *12*). The incompetent proton-transfer network of the mutant isolates the phenolic oxygen from the solvent, creating two populations of enzyme, one with the the phenolate form of pOHB that reduces quickly and the other with the phenolic form of pOHB that reduces slowly. The rapidly reducing population has the flavin in the "out" conformation, while the slowly reducing population has the flavin in the "in" conformation. It was postulated that the rate-determining step for the reduction of the slow population was deprotonation of pOHB. In this case, protein breathing would be required to effect proton transfer (*12*). Here, we show that the rate of reduction of the slow population of the His72Asn mutant is indeed determined by the rate of deprotonation of pOHB. This process was also studied in the wild-type protein, where we directly observed the involvement of the intact proton-transfer network in the reductive half-reaction.

MATERIALS AND METHODS

Wild-type PHBH from *Pseudomonas aeruginosa* and the His72Asn mutant were expressed in *Escherichia coli* and purified as described (*4*, *7*, *9*). (4*R*)-[4-^{2}H]NADPH (NADPD) was synthesized by the aldehyde dehydrogenase-catalyzed reduction of NADP with deutero-acetaldehyde followed by purification with ion-exchange chromatography (*4*). Rapid reactions were performed anaerobically (*13*) on Hi-Tech SF-61, Hi-Tech SF-61 DX2, or Kinetic Instruments stopped-flow spectrophotometers. Stopped-flow instruments were made anaerobic by washing first with anaerobic water followed by soaking for at least 10 h with an oxygen-scavenging solution of protocatechuate and protocatechuate dioxygenase and again washing with anaerobic water (*14*). Kinetic experiments were performed at 4 °C using 10−20 μM enzyme solutions (active-site concentrations after mixing). Absorbance traces were fit to sums of exponentials by Marquardt−Levenberg algorithms implemented in program A (Rong Chang, Chung-Jin Chiu, Joel Dinverno, and David P. Ballou, University of Michigan), KISS (Kinetic Instruments), or pro Fit (Quantum Soft) to obtain observed rate constants. The pH dependence of enzyme reactions was studied by exchanging the buffer of concentrated enzyme solutions with the buffer of choice using EconoPak 10-DG columns (BioRad) equilibrated in the appropriate potion. For pH values between 6 and 7.8, the buffer was 50 mM potassium phosphate; between pH 8 and 9, the buffer was 100 mM TrisSO_4; and for pH values greater than 9, the buffer was 50 mM glycine. Buffer solutions in D_2O for use in the determination of solvent kinetic isotope effects were prepared in H_2O, adjusted to the desired pH, dried by evaporation under vacuum, and redissolved in D_2O; this process was repeated at least 2 more times. Preparing buffers in this way kept the ratio of conjugate acid to conjugate base identical in H_2O and D_2O solvents (*15*). Buffer-free experiments were conducted in 50 mM Na_2SO_4 solutions whose pH was adjusted to 6.2 with dilute H_2SO_4 or NaOH after bubbling with O_2-free and CO_2-free argon and cooling to 4 °C. Extreme care was taken to ensure that the pH values of all enzyme and substrate solutions in buffer-free experiments were identical. Fluorescein-conjugated dextran (MW, 10 000; Molecular Probes, Inc.) was used as a pH indicator at concentrations of 5 μM (concentration of dye after mixing). Changes in pH were detected by observing the high fluorescence of the deprotonated dye (λ_{ex} = 491 nm, and $\lambda_{em} \geq$ 500 nm with a cutoff filter). Control experiments showed that, unlike free fluorescein, dextran-conjugated fluorescein did not bind to the enzyme.

RESULTS

Kinetic Mechanism of the Reductive Half-Reaction of His72Asn PHBH. The reductive half-reaction of the His72Asn mutant enzyme was studied by mixing anaerobic solutions of the enzyme−pOHB complex with anaerobic solutions of NADPH that also contained pOHB. Reactions were at 4 °C in buffers of pH ranging from 6.1 to 9.6. The reduction of enzyme-bound oxidized FAD was monitored by the change in absorbance at 450 nm. As reported previously, the His72Asn mutant is reduced by NADPH in two phases (*4*). The two phases were attributed to two populations of enzymes, one with the phenolate form of pOHB bound that was competent for rapid reaction with NADPH and the other with the phenolic form of pOHB bound that slowly changed conformation to the competent form prior to the reaction. However, a detailed kinetic model was not presented and is developed here.

Three possible mechanisms for the reaction of the mutant enzyme were considered. In each mechanism, NADPH binds in a rapid equilibrium to both the fast and slow forms of the enzyme and the fast form is reduced rapidly in the first reaction phase, leaving only the slow form as oxidized. The slow form of the enzyme subsequently isomerizes to the fast form and is rapidly reduced by NADPH. The three mechanisms differ in the details of the rate-determining isomerization. In mechanism 1, the rapidly reacting and slowly reacting enzyme forms interconvert only when NADPH is

Scheme 1

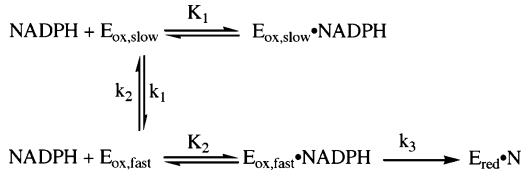

Scheme 2

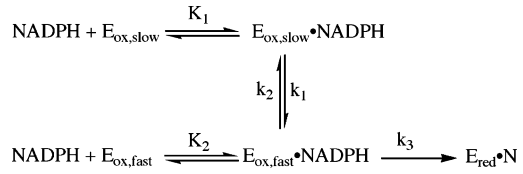

Scheme 3

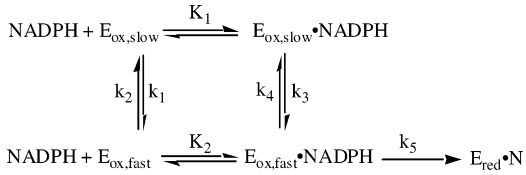

not bound (Scheme 1). In mechanism 2, the rapidly reacting and slowly reacting enzyme forms interconvert only when NADPH is bound (Scheme 2). In mechanism 3, both the rapidly and slowly reacting enzyme forms interconvert regardless of whether NADPH is bound (Scheme 3). Each mechanism predicts a simple hyperbolic NADPH concentration dependence for the observed rate constant of the first (fast) phase of reduction, but each makes a distinct prediction about the concentration dependence of the second phase, given in eqs 1−3 (see the Appendix for derivations). Mechanism 1 predicts that, as NADPH concentration increases, the observed rate constant will increase to a maximum and then decrease (eq 1). Mechanism 2 predicts a square-hyperbolic dependence that goes through the origin (eq 2). Mechanism 3 predicts a potentially complex concentration dependence (eq 3), with the possibility of an apparent nonzero intercept (analysis in the Appendix).

$$k_{obs} = \frac{k_1 k_3 K_1 [NH]}{k_3 [NH]^2 + (k_1 K_1 + k_2 K_2 + k_3 K_1)[NH] + (k_1 + k_2) K_1 K_2} \quad (1)$$

$$k_{obs} = \frac{k_1 k_3 [NH]}{(k_1 + k_2 + k_3)[NH] + k_1 K_2 + (k_2 + k_3) K_1} \quad (2)$$

$$k_{obs} = [k_3 k_5 [NH]^2 + k_1 k_5 K_1 [NH]] / [(k_3 + k_4 + k_5)[NH]^2 + ([k_1 + k_4 + k_5] K_1 + [k_2 + k_3] K_2)[NH] + (k_1 + k_2) K_1 K_2] \quad (3)$$

The observed rate constant for reduction of the FAD of the rapidly reducing population of the His72Asn−pOHB complex has a hyperbolic dependence on the NADPH concentration at all pH values, giving a reduction rate constant of 82 ± 2 s^{-1} and a K_d for NADPH of 33 ± 14 μM (*4*), consistent with the binding of NADPH followed by hydride transfer to FAD predicted by all models. The

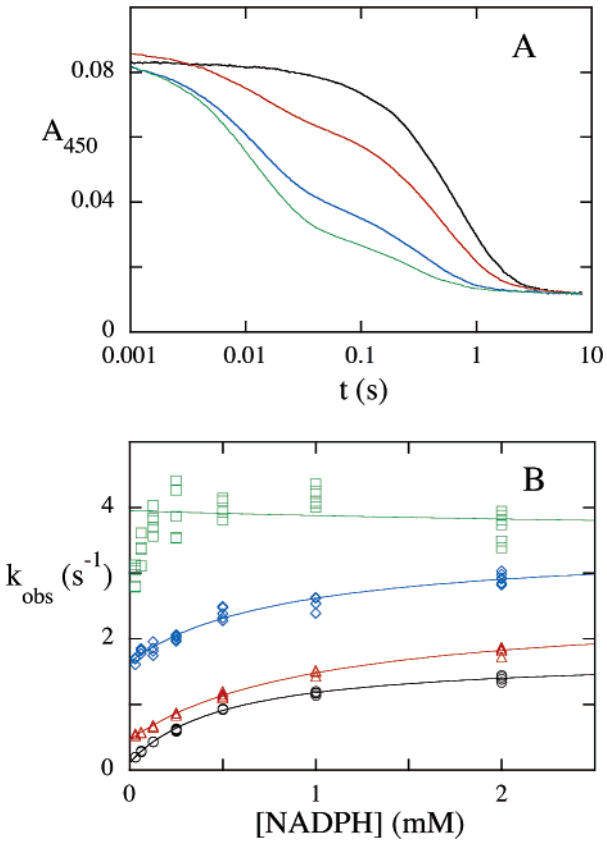

FIGURE 2: NADPH dependence of the reduction of the slow form of His72Asn. Anaerobic solutions of the His72Asn−pOHB complex were reduced by mixing with NADPH solutions in a stopped-flow spectrophotometer at 4 °C. The observed rate constants of the biphasic exponential traces were plotted as a function of the NADPH concentration. A shows reaction traces at a saturating concentration of NADPH (2 mM). Black is pH 6.5; red is pH 7.8; blue is pH 8.65; and green is pH 9.46. All traces gave excellent fits to two exponentials ($R \geq 0.99994$). Note the logarithmic time scale. B shows the observed rate constants for the slow phase of reduction obtained at pH 6.5 (black circles), pH 7.8 (red triangles), pH 8.65 (blue diamonds), and pH 9.47 (green squares). The lines for pH 6.5−8.65 represent fits to eq 4. The data obtained at pH 9.47 do not fit eq 4 at the lower NADPH concentrations, apparently because of the breakdown of one or more of the assumptions required to derive it, but appear to conform at higher concentrations. The line drawn through the pH 9.47 data represents a fit to the data using eq 4, with k_1 fixed to 3.9 s^{-1} (the value predicted from the data in ref *12*) and k_3 fixed to 3.5 s^{-1}.

observed rate constants for the slowly reducing enzyme population increased to a limiting value with increasing NADPH concentration and, importantly, extrapolated to a finite value as the NADPH concentration approached 0 (Figure 2). This concentration dependence is only consistent with mechanism 3 (Scheme 3); mechanisms 1 and 2 both predict limiting values of the observed rate constant of 0 as the NADPH concentration approaches 0. Mechanism 1 also predicts that the observed rate constant of the slow phase will reach a maximum value and then approach 0 at high NADPH concentrations because NADPH binding traps the enzyme in a form that cannot isomerize, behavior that was not observed. Furthermore, it has previously been shown in pH-jump experiments that the slow and fast enzyme forms interconvert in the absence of NADPH on the time scale of the slow reduction reaction (*12*), contradicting mechanism 2.

Table 1: Kinetic Parameters for the Isomerization of His72Asn[a]

	measured[b]			predicted[c]		calculated parameters		
pH/pD	k_1 (s^{-1})	k_3 (s^{-1})	K_1 (mM)	k_1 (s^{-1})	k_2 (s^{-1})	k_4 (s^{-1})[d]	k_3/k_1	k_4/k_2
A. H_2O								
6.55	0.11	1.73	0.52	0.13	4.6	2.3	16	0.5
7.8	0.46	2.52	1.02	0.47	1.1	0.12	5	0.1
8.65	1.64	3.4	0.8	1.9	0.93	0.042	2	0.05
9.47[e]	3.9	3.5		3.9	0.90			
B. D_2O								
7.47	0.0137	0.52	1.4	0.037	0.94	0.51	38	0.54
9.15	0.265	0.96	2.3	0.56	0.61	0.019	3.6	0.032
9.89	0.535	0.80	0.8	1.4	0.60	0.022	1.5	0.037
10.88	0.79	0.49	0.79	2.0	0.60	0.012	0.62	0.02

[a] Rate constants refer to Scheme 3 and were obtained by fitting the observed rate constants for the second reaction phase as described in the text. Reactions were at 4 °C. [b] Measured values were obtained by fitting the data in Figures 2 and 4 to eq 4 as described in the text. [c] Predicted values for k_1 and k_2 were calculated (in units of s^{-1}) using the rate laws derived from ref *12*. In H_2O, the expressions are $k_1 = 0.11 + [(4.8 \times 10^{pH-pK_w})/(1.4 \times 10^{-6} + 10^{pH-pK_w})]$ and $k_2 = 1.3 \times 10^7 \times 10^{-pH} + 0.9$, while in D_2O, the expressions are $k_1 = 0.022 + [(2.1 \times 10^{pH-pK_w})/(7.4 \times 10^{-7} + 10^{pH-pK_w})]$ and $k_2 = 1.0 \times 10^7 \times 10^{-pH} + 0.6$. The numerical values in these equations are the averages of the data given in Table 2 of ref *12*, and the functional forms come from the rate laws determined in that study for Scheme 1 in ref *12*. The value of pK_w of H_2O at 4 °C is 14.741, and the value of pK_w of D_2O at 4 °C is 15.739 (*16*). [d] The value of k_4 was calculated from the thermodynamic cycle involving the oxidized enzyme forms in Scheme 3 using $k_4 = k_3(k_2/k_1)(K_2/K_1)$. The predicted values of k_1 and k_2 listed in the table were used in the calculations. [e] Data obtained at pH 9.47 had a high degree of scatter and did not conform to eq 4. Values for k_1 and k_3 were estimated visually from the data at low and high NADPH concentrations. There was insufficient curvature to properly estimate a value for K_1.

The rate of reduction and therefore isomerization of the slow form of the enzyme was significantly lower than the rate of reaction of the fast form. Therefore, it is reasonable to suppose that, in Scheme 3, k_5 is much larger than the rate constants involved with the conformational change (k_1, k_2, k_3, and k_4). Furthermore, the apparent dissociation constant of NADPH was ~30-fold greater for the slow form of the enzyme than it was for the fast form of the enzyme. Under these circumstances, eq 3 reduces to eq 4 (see the Appendix).

$$k_{obs} = \frac{k_3[NH] + k_1K_1}{[NH] + K_1} \quad (4)$$

Three salient features of eq 4 are (1) k_2, k_4, and k_5 have no effect on k_{obs} for the slower step. This is due to the rapid reduction of the NADPH complex of the fast enzyme conformation, which competes effectively with reactions leading back to the slow conformation, making them insignificant. This prevents values of k_2 and k_4 from being determined from these data. (2) The value of k_{obs} for the slower step may either increase or decrease with an increasing concentration of NADPH, depending upon the values of k_1 and k_3. (3) The concentration of NADPH that gives half of the maximum change in k_{obs} for the slower step (either an increase or decrease) is the dissociation constant, K_1, of NADPH from the slow conformation of the enzyme. The results of fitting the data to eq 4 are shown in Figure 2 and summarized in Table 1A. Data for the reduction of the His72Asn−pOHB complex were obtained at several pH values. At the three lowest pH values (from 6.5 to 8.65), k_{obs} increased with the NADPH concentration to limiting values and excellent fits to eq 4 were obtained. At pH 9.47, the data did not conform strictly to eq 4. Instead, k_{obs} increased up to ~0.5 mM NADPH and then gradually decreased as the NADPH concentration increased from 0.5 to 2 mM, suggesting that one of the assumptions implicit in eq 4 ($k_5 \gg k_1$, k_2, k_3, and k_4, and $K_1 \gg K_2$) no longer holds at this high pH value. Further exacerbating the problem is the fact that at high pH the amount of the slow conformation is minimal, thus decreasing the reliability of the measurements of its reaction.

The isomerization of the NADPH-free enzyme, represented by k_1 and k_2, is dependent upon pH because it is related to the ionization of pOHB. This relationship has been studied in detail previously (*12*) where acid- and base-dependent reaction pathways were characterized. The rate law from that study allows values for k_1 to be calculated (in s^{-1}) as a function of pH according to eq 5, using values for the rate constants reported in ref *12* and the autoprotolysis constant of water (pK_w) of 14.741 at 4 °C (*16*).

$$k_1 = 0.11 + \frac{4.8 \times 10^{pH-pK_w}}{1.4 \times 10^{-6} + 10^{pH-pK_w}} \quad (5)$$

The values for k_1, the rate constant for the conversion of the slow form of the NADPH-free enzyme into the fast form, obtained in these studies are in excellent agreement with those predicted by eq 5 (*12*) (Table 1). The values of k_3, the conversion of the slow enzyme form to the fast form while NADPH is bound, do not vary by a large amount, ranging from 1.7 s^{-1} at pH 6.55 to 3.4 s^{-1} at pH 8.65 and an estimated value of 3.5 s^{-1} at pH 9.47. Thus, the values for the rate constants for isomerizing to the fast enzyme form are larger when NADPH is bound, especially at low pH; the ratio of k_3/k_1 decreases from 16 at pH 6.5 to 2 at pH 8.65. At pH 9.47, where the fit to eq 4 breaks down, a value of k_3 of 3.5 s^{-1} was estimated visually (Figure 2), bringing the ratio k_3/k_1 close to 1, in accordance with the nearly invariant value of k_{obs} at high NADPH concentrations. The values of K_1, the dissociation constant of NADPH from the slow form of the enzyme, did not vary systematically over the pH range studied. An average value of 0.7 ± 0.3 mM was obtained from the three lowest pH values.

Values for k_4 could not be obtained directly by fitting the concentration dependence of k_{obs} because this value is presumably much smaller than k_5, the rate constant for hydride transfer (80 s^{-1}), and, therefore, is kinetically insignificant. However, the values obtained for K_1 and k_3, combined with those obtained previously for k_1 and k_2 (*12*), allow k_4 to be calculated by considering the thermodynamic cycle defined in Scheme 3. Because the equilibrium constant for traversing a cycle must be unity, eq 6 may be written by considering the reactions from the fast enzyme−NADPH complex.

$$1 = \left(\frac{k_4}{k_3}\right)\left(\frac{k_1}{k_2}\right)\left(\frac{K_1}{K_2}\right) \quad (6)$$

As summarized in Table 1, the value of k_4 decreases with increasing pH, from 2 s^{-1} at pH 6.55 to 0.04 s^{-1} at pH 8.65. This finding is consistent with the notion that the phenolicoxygen of pOHB must be protonated to convert the rapidly reacting form of the His72Asn mutant to the slowly reacting

form. Note that the rate constant for converting the fast enzyme form into the slow enzyme form is smaller when NADPH is bound.

Kinetic Isotope Effects on the Reduction of His72Asn PHBH. The hypothesis that the fast form of the His72Asn−pOHB complex is in a conformation ready for reduction predicts that its rate constant for the reaction with NADPH is determined by the hydride transfer reaction. Conversely, the isomerization of the slow enzyme form to the fast enzyme form is hypothesized to control the rate of the slow phase of reduction. This model predicts that the first phase will exhibit a substantial primary kinetic isotope effect when NADPD is used as a substrate but that the second phase will be insensitive to isotopic substitution on the pyridine nucleotide. Furthermore, it has been shown that proton transfers to or from the phenolic oxygen of pOHB control the rate of isomerization between the fast and slow enzyme forms (*4*, *12*). Thus, a significant solvent kinetic isotope effect is predicted on the slow phase of reduction but not on the fast phase of reduction. Both of these predictions were realized. Using NADPD, an isotope effect of 7.9 ± 0.1 was found for the reduction of the fast form of the His72Asn−pOHB complex at pH 8.5 and 4 °C (Figure 3), while no difference in rates was observed for the slow form of the His72Asn−pOHB complex. The insensitivity of the slow phase of reduction to NADPD is predicted by eq 4, which does not contain the rate constant for hydride transfer (k_5), justifying the approximations used in deriving it. Therefore, the rate of reduction of the slow form is controlled by isomerization.

The kinetics of reduction of the His72Asn mutant in D_2O were determined across a range of pD values in double-mixing stopped-flow experiments at 4 °C. The anaerobic enzyme−pOHB complex, initially in a dilute buffer (5 mM Tris sulfate at pD 8.5), was mixed with an anaerobic concentrated buffer at the desired pD and allowed to age for 5 s, long enough to establish the equilibrium between the fast and slow enzyme forms (*12*). After this age time, the enzyme was mixed with an anaerobic solution of NADPH in a buffer at the appropriate pD to determine the kinetics of reduction. The rate constant for reduction of the fast form of the enzyme did not vary with pD. A solvent isotope effect of 1.07 ± 0.02 was found for the reduction of the fast form of the enzyme at all pD values (data not shown), indicating that proton transfers are not involved in this reaction. In contrast, a substantial solvent isotope effect was observed for the reaction of the slow form of the enzyme. The observed rate constant for the slow phase was measured as a function of NADPH from pD 7.47 to 10.88 and analyzed using eq 4 to obtain k_1 and k_3 as described in the previous section (Figure 4). Excellent fits to eq 4 were obtained at all pD values. Note that at the highest pD, 10.88, k_{obs} decreased with increasing NADPH, indicating that k_3 was less than k_1 under these conditions. The values obtained from fitting the data are listed in Table 1B. Note that the values for k_3 in D_2O are significantly lower than those obtained in H_2O (Table 1A). Although the lack of systematic variation prevents the meaningful calculation of an isotope effect, it is clear that this value is relatively large (> ~2) at all pL values, consistent with the notion that proton transfers are necessary to convert the slow enzyme form into the fast enzyme form.

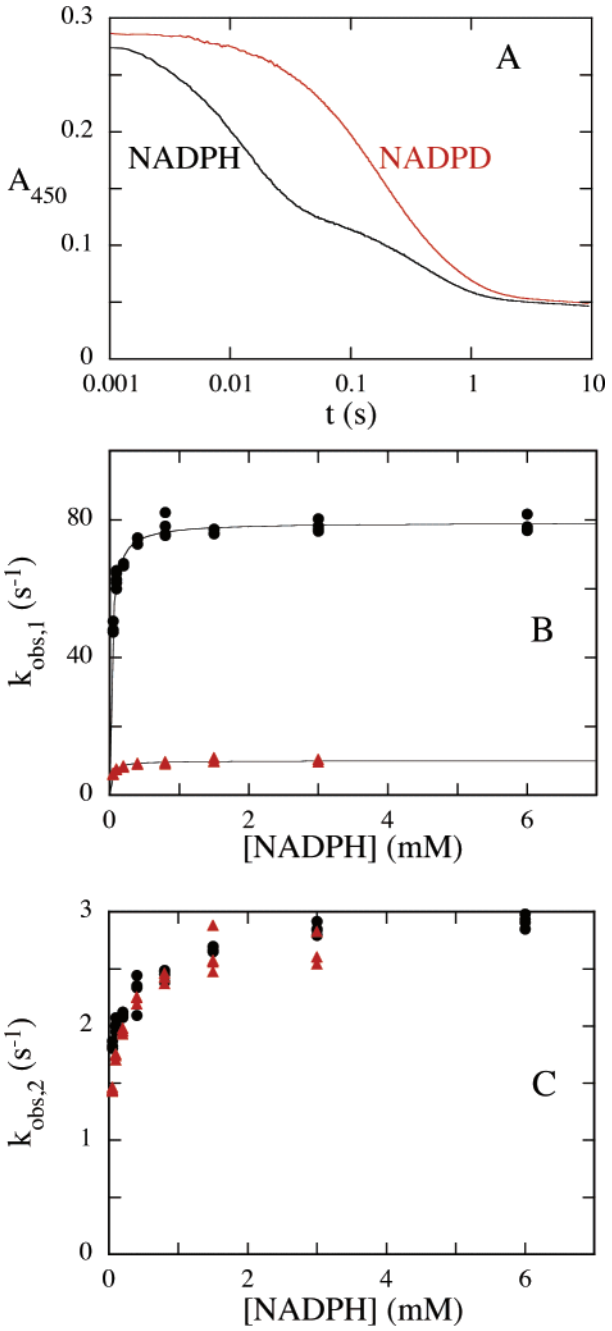

FIGURE 3: Kinetic isotope effect on the reduction of His72Asn−pOHB. Anaerobic solutions of the His72Asn−pOHB complex were reduced with anaerobic solutions of pyridine nucleotide in a stopped-flow spectrophotometer at 4 °C and pH 8.5. Reaction traces, shown in A for 3 mM NADPH (black) and 3 mM NADPD (red), were biphasic and fit to the sum of two exponentials to obtain values of k_{obs} for each phase. The values of k_{obs} for the fast phase of reduction are shown in B. An isotope effect of 7.9 was obtained from the ratio of the reduction rate constants (k_{obs} extrapolated to infinite pyridine nucleotide) for NADPH (black) and NADPD (red). The values of k_{obs} for the slow phase of reduction using NADPH (black) or NADPD (red), shown in C, showed no isotope effect.

Proton Movements Associated with the Reduction of Wild-Type PHBH. The importance of His 72 in the reduction reaction, deduced by earlier studies of the His72Asn mutant, has led to a kinetic model for coupling proton transfers in the wild-type enzyme to flavin movement and reduction. The model predicts that the phenolate of bound pOHB is required to cause the flavin to move rapidly from the "in" to the "out"

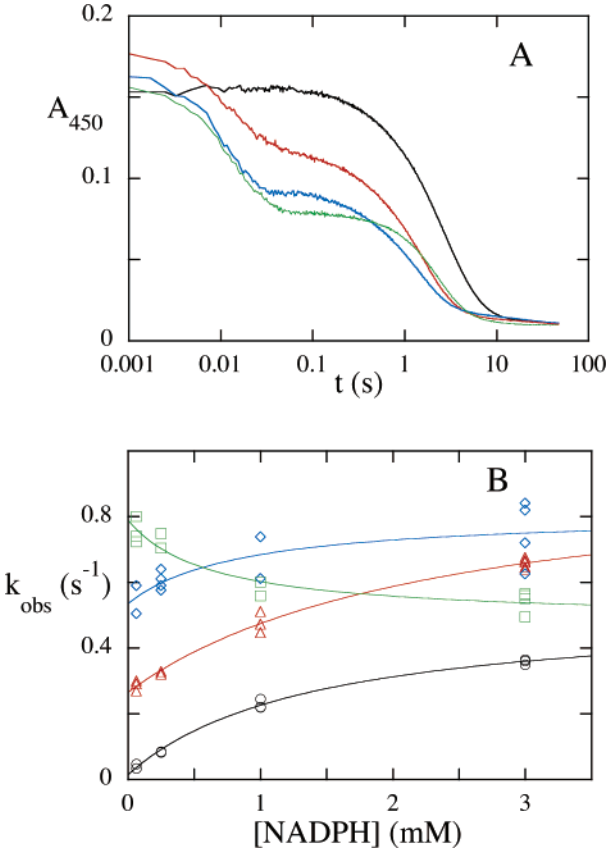

FIGURE 4: NADPH dependence of the reduction of the slow form of His72Asn in D_2O. Anaerobic solutions of the His72Asn−pOHB complex in D_2O were reduced by mixing with NADPH solutions in a stopped-flow spectrophotometer at 4 °C. The observed rate constants of the slow phase of the biphasic exponential traces are plotted as a function of the NADPH concentration. A shows reaction traces at saturating (3 mM) NADPH. Black is pD 7.47; red is pD 9.15; blue is pD 9.89; and green is pD 10.88. Note the logarithmic time scale. B shows the observed rate constants for the slow phase of reduction obtained at pD 7.47 (black circles), pD 9.15 (red triangles), pD 9.89 (blue diamonds), and pD 10.88 (green squares). The lines for pD 6.5−8.65 represent fits to eq 4.

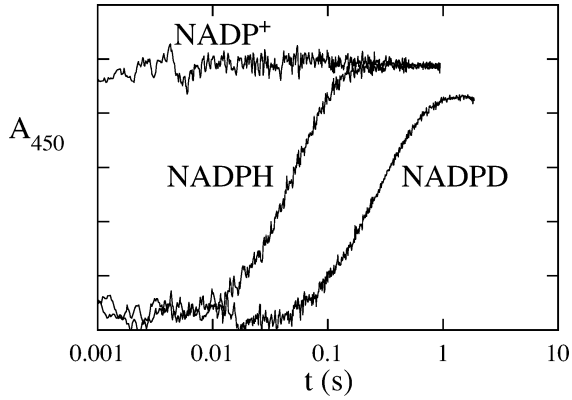

FIGURE 5: Proton movements during the reduction of wild-type PHBH. Anaerobic wild-type PHBH (35.5 μM active sites), 0.5 mM pOHB, and dextran-conjugated fluorescein (10 μM in dye) in 50 mM Na_2SO_4 at pH 6.2 and 4 °C were mixed with anaerobic unbuffered solutions of NADPH or NADPD (6 mM before mixing) in 50 mM Na_2SO_4 at pH 6.2 in a stopped-flow spectrophotometer. The fluorescence of the fluorescein dye was monitored (excitation at 491 nm and emission at wavelengths greater than or equal to 500 nm). As a control, the enzyme was also mixed with 6 mM $NADP^+$ in 50 mM Na_2SO_4 at pH 6.2, giving the flat fluorescence trace. When reduced pyridine nucleotides were used, a large loss of fluorescence occurred in the dead time of the instrument, followed by an increase in fluorescence that exhibited an isotope effect of 7.1 ± 0.5.

conformation, where it reacts with NADPH (*4*, *8*, *12*). The rapid generation of the phenolate of pOHB requires an intact proton-transfer network, and deprotonation of pOHB by the proton-transfer network is triggered by the binding of NADPH. This model predicts that at low pH, when pOHB and His 72 are both protonated, the binding of NADPH should cause the loss of a proton to solution prior to flavin reduction. Furthermore, it is thought that pOHB is in the phenolic form and the flavin is "in" after reduction (*5*), predicting that, upon reduction at low pH, a proton will be taken from solution. These predictions were tested by performing the reduction reaction without a buffer but in the presence of a pH indicator. An anaerobic solution of wild-type PHBH (35.4 μM in active sites before mixing) and 0.5 mM pOHB in 50 mM Na_2SO_4 containing fluorescein-conjugated dextran (10 μM in fluorescein) at pH 6.2 was mixed in a stopped-flow instrument with buffer-free anaerobic solutions of NADPH or NADPD and 0.5 mM pOHB in 50 mM Na_2SO_4 adjusted to pH 6.2. The fluorescein−dextran conjugate becomes highly fluorescent when deprotonated. Flavin reduction was monitored by absorbance and was found to be unaffected by the presence of the fluorescein−dextran conjugate. When observed by fluorescence (excitation at 491 nm and emission at ≥500 nm), a dead-time drop in fluorescence was observed (Figure 5), indicating that the rapid binding of NADPH caused the release of protons to the solution. The fluorescence increased to its original level with an observed rate constant of 27.4 s^{-1}, the same as that for flavin reduction. NADPD reduces wild-type PHBH with a kinetic isotope effect of 8.9 (*4*). When NADPD was used in these experiments, an isotope effect of 7.1 ± 0.5 was observed for both flavin reduction, observed by the change in flavin absorbance, and the fluorescence increase (Figure 5), demonstrating that hydride transfer controlled the rate of proton uptake.

Solvent Isotope Effects on the Reduction of Wild-Type PHBH. The model linking proton transfers to flavin reduction predicts that wild-type PHBH should exhibit a substantial solvent kinetic isotope effect when the proton-transfer network is fully protonated, but the effect should diminish at high pH values, where the proton-transfer network is deprotonated and proton transfers are unnecessary. This prediction was tested by comparing the kinetics of the reductive half-reaction in H_2O and D_2O in stopped-flow experiments. The ratio of conjugate acid and conjugate base was kept the same in D_2O to account for solvent isotope effects on pK_a values (*15*). At pH 6.55 in H_2O, 50 mM potassium phosphate buffer was used, and at pH 9.5, 0.1 M glycine was used. At the low pH, a solvent isotope effect of 2.08 ± 0.08 was found for the rate constant of flavin reduction. At the higher pH value, the solvent isotope effect decreased to 1.40 ± 0.04. These values are consistent with the model linking proton transfers from pOHB to the reduction reaction. The value of 1.4 for the deprotonated wild type is slightly higher than that of the deprotonated (fast) mutant. The basis for this difference is not clear.

Substrate Isotope Effects on Wild-Type PHBH in the Presence of D_2O. Deprotonation of the substrate via the proton-transfer network at low pH is thought to be required

Scheme 4

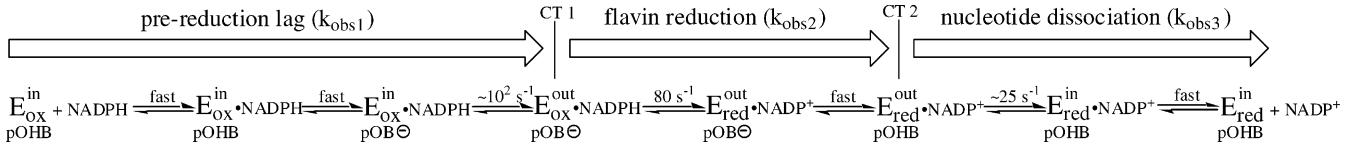

to allow the flavin to move to the "out" conformation, enabling the subsequent hydride transfer reaction. Because proton transfer and hydride transfer occur during different reaction steps, it was predicted that the value of the primary kinetic isotope effect for hydride transfer would be diminished when D_2O was the solvent because the necessary proton-transfer reaction would become more rate-determining. The reductive half-reaction was studied at pH 6.5 in H_2O and the corresponding buffer in D_2O using either NADPH or NADPD. The observed kinetic isotope effect decreased from a value of 8.9 in light water to 6.6 ± 0.5 when heavy water was the solvent, consistent with the model of proton transfers occurring prior to the hydride transfer. Analogous experiments performed at pH 9.5 produced a similar result, although the difference in primary isotope effects was smaller: an isotope effect of 9.7 ± 0.3 was found in H_2O, and an isotope effect of 8.6 ± 0.1 was found in D_2O. The smaller perturbation on the primary isotope effect indicates that the reductive half-reaction is less dependent on proton transfers at high pH, which is expected when the proton-transfer network is already deprotonated. At the higher pH, the solvent isotope effect is not likely due to proton transfers but rather to a change in hydrogen-bond strength as the reactive conformation is reached.

Viscosity Effects on the Reaction of NADPH with Wild-Type PHBH. The wild-type enzyme was reduced at pH 8.63 and 4 °C, in stopped-flow experiments that included 40% sucrose in both the enzyme and NADPH solutions. A total of 40% sucrose increases the viscosity by a factor of 9 (*17*). A rate constant for reduction of 76 ± 4 s^{-1} was determined from the variation of the observed rate constant with the NADPH concentration. This value is the same as that obtained in the absence of the viscogen. The value of the apparent dissociation constant of NADPH obtained in the presence of sucrose was 240 ± 40 μM, approximately 10-fold higher than in the absence of sucrose. The change in K_d can be attributed to the increased energy in the presence of high sucrose to change NADPH from its stacked conformation that it adopts in solution (*18*) to that required for binding. Therefore, the ratio of the reduction rate constant divided by the dissociation constant of NADPH, a lower limit on the bimolecular rate constant for binding (*19*), was 10-fold lower in the viscous solvent, indicating that NADPH binding is limited by diffusion.

DISCUSSION

The mechanisms controlling PHBH satisfy the disparate requirements of the reductive and oxidative half-reactions. While the oxidative half-reaction requires a solvent-sequestered flavin hydroperoxide, the reductive half-reaction needs the flavin to be accessible to NADPH. This is accomplished by coupling the position of the isoalloxazine moiety of the flavin to the protonation state of the aromatic substrate. In this study, we have directly observed the participation of the proton-transfer network in the reductive half-reaction. Results of the experiments presented in this report, in concert with data from previous studies mentioned below, lead to the following detailed mechanism for the reductive half-reaction (Scheme 4). NADPH associates with the PHBH·pOHB complex in a diffusion-limited manner as evidenced by the viscosity effect on reduction. Ionizing the bound substrate to an anion on the phenolic oxygen causes electrostatic repulsion with the carbonyl of Pro293 and induces the movement of the flavin to the reduction-competent "out" conformation (*8*). If the bound substrate is not ionizable, the flavin will not be reduced quickly. In the "out" conformation, the oxidized flavin makes a charge-transfer interaction with NADPH and hydride transfer occurs, forming a new charge-transfer interaction between NADP and reduced flavin (*20, 21*). Upon reduction, the reduced isoalloxazine is in the anionic form (*22*) and pOHB is protonated from the solvent via the proton-transfer network to produce the phenolic form of the substrate. The anionic flavin is drawn back into the "in" conformation by the positive electrostatic potential of the active site, and NADP dissociates rapidly. This mechanism is summarized in Scheme 4. At this point, reduced flavin is poised to react with O_2 and hydroxylate pOHB, a reaction that requires the phenolate form of pOHB (*23*). Thus, in the reductive half-reaction, the aromatic substrate is not chemically involved like it is in the oxidative half-reaction, but it is nonetheless critical.

Many of the events depicted in Scheme 4 are demonstrated by experiments with the His72Asn mutant. Because the proton-transfer network in this mutant is not functional and decouples proton transfers from flavin movement, we can directly observe the kinetic consequences on flavin reduction. The incompetent proton-transfer network of the mutant isolates the phenolic oxygen from the solvent, creating two populations of enzyme that interconvert slowly, one with the phenolate form of pOHB that reduces quickly and another with the phenolic form of pOHB that reduces slowly (*4*). The fast form exhibits a large isotope effect (7.9) in the reaction with NADPD, demonstrating that hydride transfer is rate-determining. In contrast, the slow form has no isotope effect, indicating that processes other than hydride transfer control the rate of reduction. As a probe for proton transfers, we measured solvent isotope effects. The fast form has no solvent isotope effect, whereas the slow form has a substantial solvent isotope effect, indicating that protonation/deprotonation events determine the rate of flavin reduction. The kinetic isotope effect data are consistent with steps 2−4 in Scheme 4.

The kinetics of isomerization of the His72Asn enzyme·pOHB binary complex have been studied by pH-jump experiments (*12*). The reduction experiments presented here addressed the isomerization of both the binary (enzyme·pOHB) and ternary (enzyme·pOHB·NADPH) complexes. We considered three models for isomerization: one where isomerization occurs only in the binary complex (enzyme·

pOHB), one where only the ternary complex isomerizes (enzyme·pOHB·NADPH), and one where isomerization occurs for both the binary and ternary complexes. This final model (Scheme 3) is the only one that is consistent with the data. A comparison of kinetic parameters obtained in this work with those predicted from previous pH-jump experiments (*12*) shows excellent agreement when the solvent was H_2O. The agreement is still reasonable, given the complexity of the analyses, when the solvent was D_2O. Although isomerization does occur in both the presence and absence of NADPH, NADPH pushes the equilibrium position of the flavin to favor the "out" form by both increasing the rate of isomerization to the "out" form and slowing the isomerization to the "in" form. The carbonyl of Pro293 is thought to move to allow proton transfer to pOHB in the His72Asn mutant (*12*). The presence of NADPH speeds the isomerization reaction, suggesting that it causes Pro293 to become more mobile, facilitating proton transfer from pOHB. The crystal structure of Arg220Gln PHBH reveals a novel NADPH-binding site (*24*). A model for NADPH bound to the enzyme was derived from structures of the Arg220Gln mutant. However, this model does not offer insight into the mechanism of NADPH-stimulated isomerization because the flavin in this model is already in the "out" conformation and there is no pOHB in the model.

Proton transfers were directly observed during the reduction of the wild-type enzyme. In experiments with a pH indicator, the timing of the changes in the pH of the buffer-free solution are in excellent agreement with our model for flavin reduction. In step 2, the phenolic oxygen of the bound substrate is removed by the proton-transfer network, causing a rapid (dead time) decrease in pH upon NADPH binding (Figure 5). In step 6, the anionic reduced flavin moves back to the "in" position. This is accompanied by reprotonation of pOHB by the proton-transfer network, causing the observed return of the solution to its original pH. Flavin reduction and proton uptake are linked, as demonstrated by the significant and identical NADPD isotope effects on both flavin reduction and proton uptake. As would be predicted from the model, there is a substantial solvent isotope effect on flavin reduction (2.08) at low pH. Proton uptake and hydride transfer occur in separate steps, as demonstrated by the change of the substrate isotope effect at low pH from 8.9 in H_2O to 6.6 in D_2O. If the reaction were concerted, the isotope effect observed for the transfer of one hydrogen would not be changed by the isotopic composition of the other hydrogen. However, we observed an isotope effect on an isotope effect, indicating stepwise hydride and proton transfer. At high pH, where the pOHB was already deprotonated, the solvent KIE with NADPH as a substrate was smaller (1.40). Nevertheless, a solvent isotope effect on the substrate isotope effect (9.7 in H_2O and 8.6 in D_2O) was still observed. We attribute this to changes in hydrogen bonding in steps other than hydride transfer. The substrate isotope effects for the wild-type enzyme were large at both pH extremes, indicating that proton transfers are never fully rate-determining when the proton-transfer network is intact.

The results presented here and elsewhere (*3*, *4*, *8*, *12*, *19*) highlight the intricate control mechanism that has evolved for controlling flavin reduction in PHBH. The enzyme avoids wastefully consuming NADPH in the absence of pOHB by preventing flavin movement to the "out" conformation, where reduction occurs, unless pOHB is bound to the enzyme. The negative charge that can be generated by the enzyme on the aromatic ligand triggers the conformational change of the flavin, enabling reduction and discriminating against a likely competitor, *p*-aminobenzoate. PHBH has adapted the proton-transfer network, required chemically for the hydroxylation reaction, to the task of ligand recognition via ionization. Deprotonation of pOHB by this network is stimulated by the binding of NADPH. The phenolate generated on pOHB by the proton-transfer network and the binding of NADPH cause flavin movement by creating repulsion at the peptide carbonyl of Pro 293, allowing reduction (*8*). In addition to flavin movement, there is evidence that ligand ionization may cause other structural effects that stimulate the reduction reaction (*21*). The reductive half-reactions of all flavoprotein aromatic hydroxylases studied to date are stimulated to some extent by the binding of the aromatic substrate (*25*). It appears that the proton-transfer network used by PHBH represents only one of the possible methods for controlling flavin reduction. There is no evidence from sequence alignments that enzymes other than pOHB have such a network (*12*), and the only other structure of a flavoprotein aromatic hydroxylase to be determined, that of phenol hydroxylase, lacks an analogous network, although it too moves the isoalloxazine moiety of FAD from "in" to "out" to control reduction (*11*, *26*). Thus, while all members of the family of flavoprotein aromatic hydroxylases appear to control their reductive half-reactions by flavin movement, the molecular mechanisms controlling the position of the flavin are probably diverse. This is not surprising, given the disparate roles of flavoprotein aromatic hydroxylases in metabolism, where it is likely that the control of catalysis of each of these enzymes will be subject to the selective demands unique to its biological niche, the structures of the substrate and possible competitors, and the physiological tolerance for catalytic promiscuity.

APPENDIX

Derivation of Expressions for the Observed Rate Constant of Reduction for the Slow Enzyme Population. Three mechanisms were considered for the reaction of the slow form of the His72Asn mutant enzyme: (1) only the NADPH-free enzyme forms can interconvert; (2) only the NADPH-bound forms can interconvert; and (3) both NADPH-free and NADPH-bound forms interconvert. In all cases, NADPH is assumed to bind in a rapid equilibrium. It is also assumed that the population of the enzyme in the rapidly reacting conformation reacts completely in the first reaction phase before a significant proportion of the slow population reacts, so that, at the start of the second reaction phase, only the enzyme in the slow conformation is present. In the following schemes and derivations, the enzyme forms that are in the rapidly reacting conformation are designated by a subscript "f", those in the slowly reacting conformation are designated by a subscript "s", NADPH and NADP are abbreviated "NH" and "N", respectively, and reduced enzyme is denoted with a subscript "red". All equilibrium constants in these schemes are dissociation constants.

Mechanism 1: Only NADPH-Free Forms Can Interconvert. This mechanism is shown in Scheme A1. Because NADPH binding is assumed to be a rapid equilibrium, the scheme can be replaced with a simpler equivalent (*27*) shown

Scheme A1

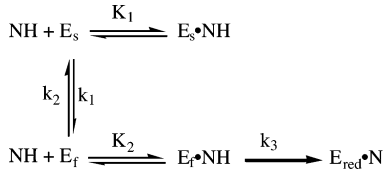

Scheme A2

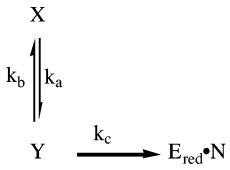

Scheme A3

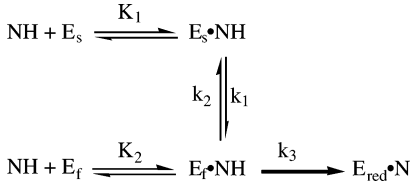

in Scheme A2, where *X* represents the pool of rapidly equilibrating slow enzyme forms, *Y* represents the pool of rapidly equilibrating fast enzyme forms, and rate constants k_a, k_b, and k_c are k_1, k_2, and k_3, respectively, modulated by the fraction of enzyme, f, in a form capable of reacting and are given in eqs A1−A3.

$$k_a = f_{E_s} k_1 = \frac{K_1 k_1}{K_1 + [NH]} \quad (A1)$$

$$k_b = f_{E_f} k_2 = \frac{K_2 k_2}{K_2 + [NH]} \quad (A2)$$

$$k_c = f_{E_f NH} k_3 = \frac{[NH] k_3}{K_2 + [NH]} \quad (A3)$$

Scheme A2 is described by the following differential equations:

$$\frac{dX}{dt} = -k_a X + k_b Y \quad (A4)$$

$$\frac{dY}{dt} = k_a X - (k_b + k_c) Y \quad (A5)$$

$$\frac{d[E_{red}N]}{dt} = k_c Y \quad (A6)$$

To solve for the time dependence of $[E_{red}N]$, *Y* will be assumed to be in a steady-state, giving

$$k_a X - (k_b + k_c) Y = 0 \quad (A7)$$

Mass conservation and the assumption that Y_0 has reacted in the fast reaction phase requires that during the slow phase

$$X_0 = X + Y + [E_{red}N] \quad (A8)$$

Combining eqs A7 and A8 gives the steady-state concentration of *Y*

$$Y = \frac{k_a X_0 - k_a [E_{red}N]}{k_a + k_b + k_c} \quad (A9)$$

Equation A9 can be substituted into eq A6 to give a solvable first-order differential equation in one time-dependent variable

$$\frac{d[E_{red}N]}{dt} = \frac{k_a k_c X_0}{k_a + k_b + k_c} - \frac{k_a k_c}{k_a + k_b + k_c} [E_{red}N] \quad (A10)$$

Equation A10 can be solved, giving for the slow phase

$$[E_{red}N] = X_0 (1 - e^{-k_{obs} t}) \quad (A11)$$

where

$$k_{obs} = \frac{k_a k_c}{k_a + k_b + k_c} = \frac{k_1 k_3 K_1 [NH]}{k_3 [NH]^2 + (k_1 K_1 + k_2 K_2 + k_3 K_1)[NH] + (k_1 + k_2) K_1 K_2} \quad (A12)$$

Note the asymptotic behavior of k_{obs} in mechanism 1

$$\lim_{[NH] \to 0} k_{obs} = 0 \quad (A13)$$

$$\lim_{[NH] \to \infty} k_{obs} = 0 \quad (A14)$$

Thus, at very high and very low values of [NH], k_{obs} approaches 0. When the derivative of eq A12 with respect to [NH] was set to 0, with respect to [NH], it can be shown that k_{obs} attains a maximum value at an intermediate value of [NH]

$$k_{obs,max} = \frac{k_1 k_3 K_1}{(k_1 + k_3) K_1 + k_2 K_2 + 2\sqrt{k_3 (k_1 + k_2) K_1 K_2}} \quad (A15)$$

$$[NH]_{max} = \sqrt{\frac{(k_1 + k_2) K_1 K_2}{k_3}} \quad (A16)$$

Mechanism 2: Only NADPH-Bound Forms Can Interconvert. This mechanism is shown in Scheme A3, and after assuming rapid-equilibrium binding, it also reduces to the equivalent mechanism shown in Scheme A2, but with the definitions of k_a, k_b, and k_c given in eqs A17−A19.

$$k_a = f_{E_s} k_1 = \frac{k_1 [NH]}{K_1 + [NH]} \quad (A17)$$

$$k_b = f_{E_f NH} k_2 = \frac{k_2 [NH]}{K_2 + [NH]} \quad (A18)$$

$$k_c = f_{E_f NH} k_3 = \frac{k_3 [NH]}{K_2 + [NH]} \quad (A19)$$

Scheme A4

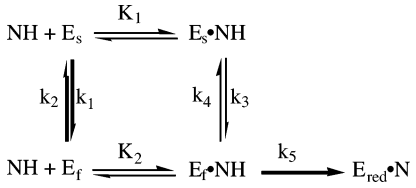

The differential equations describing Scheme A2 and the solution for $[E_{red}N]$ are given in eqs A4−A11. In mechanism 2, k_{obs} is given by

$$k_{obs} = \frac{k_1 k_3 [NH]}{(k_1 + k_2 + k_3)[NH] + k_1 K_2 + (k_2 + k_3) K_1} \quad \text{(A20)}$$

The limiting behavior in this mechanism follows

$$\lim_{[NH]\to 0} k_{obs} = 0 \quad \text{(A21)}$$

$$\lim_{[NH]\to \infty} k_{obs} = \frac{k_1 k_3}{k_1 + k_2 + k_3} \quad \text{(A22)}$$

Mechanism 3: Both Forms Interconvert. This mechanism is shown in Scheme A4, and its kinetic equivalent is again in Scheme A2. In this mechanism, k_a, k_b, and k_c are given in eqs A23−A25

$$k_a = f_{E_s} NH k_3 + f_{E_s} k_1 = \frac{k_3 [NH]}{K_1 + [NH]} + \frac{k_1 K_1}{K_1 + [NH]} \quad \text{(A23)}$$

$$k_b = f_{E_f} k_2 + f_{E_f} NH k_4 = \frac{k_2 K_2}{K_2 + [NH]} + \frac{k_4 [NH]}{K_2 + [NH]} \quad \text{(A24)}$$

$$k_c = f_{E_f} NH k_5 = \frac{k_5 [NH]}{K_2 + [NH]} \quad \text{(A25)}$$

giving

$$k_{obs} = [k_3 k_5 [NH]^2 + k_1 k_5 K_1 [NH]] / [(k_3 + k_4 + k_5)[NH]^2 + ([k_1 + k_4 + k_5] K_1 + [k_2 + k_3] K_2)[NH] + (k_1 + k_2) K_1 K_2], \quad \text{(A26)}$$

with the following limiting behavior:

$$\lim_{[NH]\to 0} k_{obs} = 0 \quad \text{(A27)}$$

$$\lim_{[NH]\to \infty} k_{obs} = \frac{k_3 k_5}{k_3 + k_4 + k_5} \quad \text{(A28)}$$

The concentration dependence of k_{obs} is not hyperbolic. However, at sufficiently high values of [NH], the first two terms in the denominator of eq A26 become much larger than the constant term and the expression reduces to

$$k_{obs} = \frac{k_3 k_5 [NH] + k_1 k_5 K_1}{(k_3 + k_4 + k_5)[NH] + (k_2 K_2 + [k_4 + k_5] K_1)} \quad \text{(A29)}$$

Therefore, within the regime of "high" [NH], k_{obs} will appear to extrapolate to a finite value as [NH] decreases

$$\lim_{[NH]\to 0} k_{obs} = \frac{k_1 k_5 K_1}{k_2 K_2 + (k_4 + k_5) K_1} \quad \text{(A30)}$$

Note that the limiting value of k_{obs} at high [NH] (eq A28) may be either higher or lower than the apparent limit as [NH] approaches 0 (eq A30), depending upon the values of the expressions in eqs A28 and A30. In our experiments with the mutant enzyme, the isomerization reaction was substantially slower than the reduction reaction; i.e., k_5 was much greater than the other rate constants. Also, the binding of NADPH was much tighter to the fast form than to the slow form, so that $K_1 \gg K_2$. Applying these approximations to eqs A28 and A30 gives

$$\lim_{[NH]\to \infty} k_{obs} = k_3 \quad \text{(A31)}$$

$$\lim_{[NH]\to 0} k_{obs} = k_1 \quad \text{(A32)}$$

and the k_{obs} value at intermediate concentrations is given by

$$k_{obs} = \frac{k_3 [NH] + k_1 K_1}{[NH] + K_1} \quad \text{(A33)}$$

Therefore, when $k_3 > k_1$, k_{obs} will increase with [NH] and, when $k_3 < k_1$, k_{obs} will decrease with increasing [NH]. Under these conditions, k_{obs} is insensitive to the values of k_2, k_4, and k_5.

ACKNOWLEDGMENT

We thank Professors David P. Ballou and Vincent Massey, University of Michigan, for providing the facilities that made this work possible, Drs. Barrie Entsch and David Ballou for helpful comments on this paper, and Professor G. Robert Greenberg for the gift of the deuterium oxide.

REFERENCES

1. Entsch, B., and van Berkel, W. J. (1995) Structure and mechanism of *para*-hydroxybenzoate hydroxylase, *FASEB J.* 476−483.
2. Husain, M., and Massey, V. (1979) Kinetic studies on the reaction of *p*-hydroxybenzoate hydroxylase. Agreement of steady state and rapid reaction data, *J. Biol. Chem. 254*, 6657−6666.
3. Palfey, B. A., Ballou, D. P., and Massey, V. (1997) Flavin conformational changes in the catalytic cycle of *p*-hydroxybenzoate hydroxylase substituted with 6-azido and 6-amino flavin adenine dinucleotide, *Biochemistry 36*, 15713−15723.
4. Palfey, B. A., Moran, G., Entsch, B., Ballou, D. P., and Massey, V. (1999) Substrate recognition by "password" in *p*-hydroxybenzoate hydroxylase, *Biochemistry 38*, 1153−1158.
5. Palfey, B. A., Frederick, K. K., Basu, R., Xu, D., Ballou, D. P., Massey, V., Moran, G., and Entsch, B. (1999) Wavin flavins and passwords: Dynamics and control in the reactions of *p*-hydroxybenzoate hydroxylase, in *Flavins and Flavoproteins* (Ghisla, S., Kroeneck, P., Macheroux, P., and Sund, H., Eds.) pp. 351−358, Rudolph Weber Agency for Scientific Publications, Berlin, Germany.
6. Schreuder, H. A., Prick, P. A. J., Wierenga, R. K., Vriend, G., Wilson, K. S., Hol, W. G. J., and Drenth, J. (1989) Crystal structure of the *p*-hydroxybenzoate hydroxylase−substrate complex refined at 1.9 Å resolution. Analysis of the enzyme−substrate and enzyme−product complexes, *J. Mol. Biol. 208*, 679−696.
7. Palfey, B. A., Entsch, B., Ballou, D. P., and Massey, V. (1994) Changes in the catalytic properties of *para*-hydroxybenzoate hydroxylase caused by the mutation Asn300Asp, *Biochemistry 33*, 1545−1554.

8. Palfey, B. A., Basu, R., Frederick, K. K., Entsch, B., and Ballou, D. P. (2002) The role of protein flexibility in the catalytic cycle of *p*-hydroxybenzoate hydroxylase elucidated by the Pro293Ser mutant, *Biochemistry 41*, 8438−8446.
9. Gatti, D. L., Palfey, B. A., Lah, M. S., Entsch, B., Massey, V., Ballou, D. P., and Ludwig, M. L. (1994) The mobile flavin of 4-OH benzoate hydroxylase, *Science 266*, 110−114.
10. Schreuder, H. A., Mattevi, A., Obmolova, G., Kalk, K. H., Hol, W. G. J., van der Bolt, F. J. T., and van Berkel, W. J. H. (1994) Crystal structures of wild-type *p*-hydroxybenzoate hydroxylase complexed with 4-aminobenzoate, 2,4-dihydroxybenzoate, and 2-hydroxy-4-aminobenzoate and of the Tyr222Ala mutant complexed with 2-hydroxy-4-aminobenzoate. Evidence for a proton channel and a new binding mode of the flavin ring, *Biochemistry 33*, 10161−10170.
11. Enroth, C., Neujahr, H., Schneider, G., and Lindqvist, Y. (1998) The crystal structure of phenol hydroxylase in complex with FAD and phenol provides evidence for a concerted conformational change in the enzyme and its cofactor during catalysis, *Structure 6*, 605−617.
12. Frederick, K. K., Ballou, D. P., and Palfey, B. A. (2001) Protein dynamics control proton transfers to the substrate on the His72Asn mutant of *p*-hydroxybenzoate hydroxylase, *Biochemistry*, *40*, 3891−3899.
13. Palfey, B. A. (2003) Time-resolved spectral analysis, in *Kinetic Analysis of Macromolecules: A Practical Approach* (Johnson, K. A., Ed.) Chapter 9, pp 203−228, Oxford University Press, New York.
14. Patil, P. V., and Ballou, D. P. (2000) The use of protocatechuate dioxygenase for maintaining anaerobic conditions in biochemical experiments, *Anal. Biochem. 286*, 187−192.
15. Quinn, D. M., and Sutton, L. D. (1991) Theoretical basis and mechanistic utility of solvent isotope effects, in *Enzyme Mechanism from Isotope Effects* (Cook, P. F., Ed.) Chapter 3, pp 73−126, CRC Press, Boca Raton, FL.
16. Bütikofer, H. P., Covington, A. K., and Evans, D. A. (1979) New data analysis method for the evaluation of ionization constants and other thermodynamic functions from the temperature dependence of the electromotive force of cells, *Electrochim. Acta 24*, 1071−1079.
17. Mathlouthi, M., and Génotelle, J. (1995) *SUCROSE Properties and Applications* (Mathlouthi, M., and Reiser, P., Eds.) pp 126−154, Blackie Academic and Professional, London, U.K.
18. Weber, G. (1957) Intramolecular transfer of electronic energy in dihydro diphosphopyridine nucleotide, *Nature 180*, 1409−1410.
19. Fersht, A. (1999) *Structure and Mechanism in Protein Science*, p 116, W. H. Freeman and Company, New York.
20. Howell, L. G., Spector, T., and Massey, V. (1972) Purification and properties of *p*-hydroxybenzoate hydroxylase from *Pseudomonas fluorescens*, *J. Biol. Chem. 247*, 4340−4350.
21. Ortiz-Maldonado, M., Entsch, B., and Ballou, D. P. (2003) Conformational changes combined with charge-transfer interactions are essential for reduction in catalysis by *p*-hydroxybenzoate hydroxylase, *Biochemistry 42*, 11234−11242.
22. Vervoort, J., van Berkel, W. J., Muller, F., and Moonen, C. T. (1991) NMR studies on *p*-hydroxybenzoate hydroxylase from *Pseudomonas fluorescens* and salicylate hydroxylase from *Pseudomonas putida*, *Eur. J. Biochem. 200*, 731−738.
23. Entsch, B., Palfey, B. A., Ballou, D. P., and Massey, V. (1991) Catalytic function of tyrosine residues in *para*-hydroxybenzoate hydroxylase as determined by the study of site-directed mutants, *J. Biol. Chem. 266*, 17341−17349.
24. Wang, J., Ortiz-Malsanado, M., Entsch, B., Massey, V., Ballou, D. P., and Gatti, D. L. (2002) Protein and ligand dynamics in 4-hydroxybenzoate hydroxylase, *Proc. Natl. Acad. Sci. U.S.A. 99*, 608−613.
25. Palfey, B. A., and Massey, V. (1998) Flavin-dependent enzymes, in *Comprehensive Biological Catalysis* (Sinnott, M., Ed.) Chapter 29, Vol. 3 (Radical reactions and oxidation/reduction), pp 83−154, Academic Press, New York.
26. Xu, D., Ballou, D. P., and Massey, V. (2001) Studies of the mechanism of phenol hydroxylase: Mutants Tyr289Phe, Asp54Asn, and Arg281Met, *Biochemistry 40*, 12369−12378.
27. Cha, S. (1968) A simple method for derivation of rate equations for enzyme-catalyzed reactions under the rapid equilibrium assumption or combined assumptions of equilibrium and steady state, *J. Biol. Chem. 243*, 820−825.

BI051119T